
DRAFT

CMS Paper

The content of this note is intended for CMS internal use and distribution only

2009/08/25

Archive Id: 1.3

Archive Date: 2009/08/20 18:18:16

Measurement of the Dijet Production Ratio in pp Collisions at 10 TeV

The CMS Collaboration

Abstract

We present an early paper draft, which contains only simulation and theory, but what follows is written as if it were reporting a real measurement of early CMS data.

We have used 10 pb^{-1} of integrated luminosity from the CMS experiment at the Large Hadron Collider at CERN to measure the dijet production ratio in two regions of jet pseudorapidity. The dijet ratio, $N(|\eta| < 0.7)/N(0.7 < |\eta| < 1.3)$, is sensitive to dijet angular distributions. The dijet ratio is measured for dijet mass values between 0.4 and 3.4 TeV and is consistent with the predictions of Quantum Chromodynamics. We exclude at the 95% confidence level the following models of new physics: quark contact interactions with scale $\Lambda < 4.0 \text{ TeV}$ and excited quarks with mass $M < 1.6 \text{ TeV}$.

This box is only visible in draft mode. Please make sure the values below make sense.

PDFAuthor:	Regina Demina, Amnon Harel, Robert Harris, Daniel Carl Miner, Marek Zielinski
PDFTitle:	Measurement of the Dijet Production Ratio in pp Collisions at 10 TeV
PDFSubject:	CMS
PDFKeywords:	CMS, physics, software, computing

Please also verify that the abstract does not use any user defined symbols

1 Within the standard model events with two energetic jets (dijets) are expected to arise in proton-
 2 proton collisions from parton-parton scattering. The outgoing scattered partons manifest them-
 3 selves as hadronic jets. The pseudorapidity, η , of the observed jets is predicted by the angular
 4 distribution of the scattered partons in Quantum Chromodynamics (QCD). New physics be-
 5 yond the standard model often produces more isotropic angular distributions than QCD, re-
 6 sulting in dijets at lower absolute values of pseudorapidity than predicted by QCD. The dijet
 7 ratio, $N(|\eta| < 0.7)/N(0.7 < |\eta| < 1.3)$, is the number of events with both jets in the region
 8 $|\eta| < 0.7$ divided by the number of events with both jets in the region $0.7 < |\eta| < 1.3$. Since
 9 many sources of systematic uncertainty cancel in this ratio, the dijet ratio is a precise test of
 10 QCD and is sensitive to new physics. A similar dijet ratio was measured at the Tevatron [1]
 11 and used to set a limit on quark contact interactions. In this paper we report a measurement of
 12 the dijet ratio as a function of dijet mass with the Compact Muon Solenoid (CMS) detector at
 13 the CERN Large Hadron Collider, with a proton-proton collision energy of $\sqrt{s} = 10$ TeV.

14 The measured dijet ratio is used to search for two models of new physics which are motivated
 15 by the possibility that quarks are composite particles. The first model is a contact interaction [2]
 16 among left-handed quarks at an energy scale Λ in the process $qq \rightarrow qq$. This is modeled with
 17 the effective Lagrangian $L_{qq} = (\pm 2\pi/\Lambda^2)(\bar{q}_L \gamma^\mu q_L)(\bar{q}_L \gamma_\mu q_L)$ with $+$ chosen for the sign. The
 18 second model is a dijet resonance coming from an excited quark [3] (q^*) in the process $qg \rightarrow$
 19 $q^* \rightarrow qg$.

20 A detailed description of the CMS experiment can be found elsewhere [4, 5]. The CMS coordi-
 21 nate system has the origin at the center of the detector, z-axis points along the beam direction
 22 toward the west, with the transverse plane perpendicular to the beam. We define ϕ to be the
 23 azimuthal angle, θ to be the polar angle and the pseudorapidity as $\eta \equiv -\ln(\tan[\theta/2])$. The
 24 central feature of the CMS apparatus is a superconducting solenoid, of 6 m internal diame-
 25 ter. Within the field volume are the silicon pixel and strip tracker, and the barrel and endcap
 26 calorimeters ($|\eta| < 3$): a crystal electromagnetic calorimeter (ECAL) and a brass-scintillator
 27 hadronic calorimeter (HCAL). Outside the field volume, in the forward region, there is an iron-
 28 quartz fiber hadronic calorimeter ($3 < |\eta| < 5$). The HCAL and ECAL cells are grouped into
 29 towers, projecting radially outward from the origin, for triggering purposes and to facilitate the
 30 jet reconstruction. In the region $|\eta| < 1.74$ these projective calorimeter towers have segmenta-
 31 tion $\Delta\eta = \Delta\phi = 0.087$, and the η and ϕ width increases at higher values of η . The cell energies
 32 above the noise suppression thresholds in the HCAL and ECAL within each projective tower
 33 are summed to find the calorimeter tower energy. Towers with $|\eta| < 1.3$ contain only cells
 34 from the barrel calorimeters, towers in the transition region $1.3 < |\eta| < 1.5$ contain a mixture
 35 of barrel and endcap cells, and towers in the region $1.5 < |\eta| < 3.0$ contain only cells from the
 36 endcap calorimeters.

37 Jets are reconstructed using the seedless infrared safe cone algorithm with cone size $R =$
 38 $\sqrt{(\Delta\eta)^2 + (\Delta\phi)^2} = 0.7$ [6]. Below we will discuss three types of jets: reconstructed, corrected
 39 and generated. The reconstructed jet energy, E , is defined as the scalar sum of the calorimeter
 40 tower energies inside the jet. The jet momentum, \vec{p} , is the corresponding vector sum: $\vec{p} = \sum E_i \hat{u}_i$
 41 with \hat{u}_i being the unit vector pointing from the origin to the energy deposition E_i inside the
 42 cone. The jet transverse momentum, p_T , is the component of \vec{p} in the transverse plane. The E
 43 and \vec{p} of a reconstructed jet are then corrected for the non-linear response of the calorimeter to a
 44 generated jet. Generated jets come from applying the same jet algorithm to the Lorentz vectors
 45 of stable generated particles before detector simulation. The corrections are chosen so that, on
 46 average, the p_T of a corrected jet is equal to the p_T of the corresponding generated jet. The
 47 corrections estimated from a GEANT [7] simulation of the CMS detector increase the average
 48 jet p_T by roughly 50% (10%) for 70 GeV (3 TeV) jets in the region $|\eta| < 1.3$. Further details on jet

49 reconstruction and jet energy corrections can be found elsewhere [8, 9]. The jet measurements
 50 presented here are within the region $|\eta| < 1.3$, where the sensitivity to new physics is expected
 51 to be the highest, and where the reconstructed jet response variations as a function of η are both
 52 moderate and smooth.

53 The dijet system is composed of the two jets with the highest p_T in an event (leading jets), and
 54 the dijet mass is given by $m = \sqrt{(E_1 + E_2)^2 - (\vec{p}_1 + \vec{p}_2)^2}$. For both leading jets required to have
 55 pseudorapidity $|\eta| < 1.3$, the estimated dijet mass resolution varies from 9% at a dijet mass of
 56 0.7 TeV to 4.5% at 5 TeV. We use data from the 2009-2010 running period corresponding to an
 57 integrated luminosity of 10 pb^{-1} . The sample we use for this search was collected by requiring
 58 at least one jet in the high level trigger with $p_T > 110 \text{ GeV}/c$. The trigger efficiency, measured
 59 from a sample acquired with a prescaled trigger with a lower p_T threshold, was greater than
 60 99% for dijet mass above $420 \text{ GeV}/c^2$. Backgrounds from cosmic rays, beam halo, and detector
 61 noise are expected to occasionally produce events with large or unbalanced energy depositions.
 62 They are removed by requiring $\cancel{E}_T / \sum E_T < 0.3$ and $\sum E_T < 10 \text{ TeV}$, where \cancel{E}_T ($\sum E_T$) is the
 63 magnitude of the vector (scalar) sum of the transverse energies measured by all calorimeter
 64 towers in the event. This cut is more than 99% efficient for both QCD jet events and the signals
 65 of new physics considered. In the high p_T region relevant for this search, jet reconstruction is
 66 fully efficient.

67 In Fig. 1 we present the observed number of dijet events as a function of dijet mass in two
 68 regions of jet pseudorapidity. We plot the events in bins approximately equal to the dijet mass
 69 resolution.

70 In Fig. 2 and table 1 we present the dijet ratio, which is the ratio of the two distributions shown
 71 in Fig. 1. The error bars shown in Fig. 2 and listed in table 1 are the 68% confidence intervals
 72 for the ratio of Poisson distributed means [10, 11]. These statistical errors are the dominant
 73 experimental uncertainty at high dijet mass. The systematic uncertainty on the measured ratio
 74 arises predominantly from the uncertainty in the relative jet energy correction between the re-
 75 gion $|\eta| < 0.7$ and $0.7 < |\eta| < 1.3$. The relative jet correction is measured directly from the dijet
 76 data using the p_T balance method [12]. While the absolute jet energy correction in either region
 77 has an uncertainty of 10%, which cancels in the ratio, the relative jet correction between the two
 78 regions has an uncertainty of 1%. The resulting systematic uncertainty in the ratio, shown in
 79 Fig. 2, varies from 0.02 to 0.04, increasing smoothly with dijet mass. The data is compared to
 80 a QCD prediction from PYTHIA [13] which includes a simulation of the CMS detector and the
 81 jet energy corrections. The data is also compared with a full QCD prediction at next-to-leading
 82 order [14]. Both predictions use CTEQ6 parton distributions [15] and a renormalization scale
 83 $\mu = p_T$. The spread of the predictions is an indication of the theoretical uncertainties in the
 84 dijet ratio. The data agrees with the general expectation from the QCD predictions that the
 85 dijet ratio should have the value 0.5.

86 In Fig. 3 we compare our data with three predictions from PYTHIA: QCD alone, QCD plus a
 87 contact interaction with scale $\Lambda = 3 \text{ TeV}$, and QCD plus an excited quark with mass $M = 1$
 88 TeV. Fig. 3 shows that the dijet ratio from the two models of new physics is significantly larger
 89 than the data. We performed a statistical comparison of the data with the two models of new
 90 physics for various values of Λ and M . The dijet ratio data excludes at 95% confidence level
 91 contact interactions with scale $\Lambda < 4.0 \text{ TeV}$ and excited quarks with mass $M < 1.6 \text{ TeV}$. This
 92 extends the previous exclusions of $\Lambda < 2.7 \text{ TeV}$ [1] and $M < 0.87 \text{ TeV}$ [16] set by experiments
 93 at the Tevatron.

94 In conclusion, we have reported the first measurement of the dijet ratio in pp collisions at $\sqrt{s} =$
 95 10 TeV. The dijet ratio is consistent with the predictions of QCD and has been used to set limits

96 on models of new physics.

97 We thank the technical and administrative staffs at CERN and other CMS Institutes, and ac-
98 knowledge support from: FMSR (Austria); FNRS and FWO (Belgium); CNPq and FAPERJ
99 (Brazil); MES (Bulgaria); CERN; CAS and NSFC (China); MST (Croatia); University of Cyprus
100 (Cyprus); Academy of Sciences and NICPB (Estonia); Academy of Finland, ME and HIP (Fin-
101 land); CEA and CNRS/IN2P3 (France); BMBF and DESY (Germany); GSRT (Greece); NKTH
102 (Hungary); DAE and DST (India); IPM (Iran); UCD (Ireland); INFN (Italy); KICOS (Korea);
103 CINVSTAV, CONACYT and UASLP-FAI (Mexico); PAEC (Pakistan); SCSR (Poland); FCT
104 (Portugal); JINR (Armenia, Belarus, Georgia, Ukraine, Uzbekistan); MST and MAE (Russia);
105 MSEP (Serbia); OCT (Spain); ETHZ, PSI, University of Zurich (Switzerland); NSC (Taipei);
106 TUBITAK and TAEK (Turkey); STFC (United Kingdom); DOE and NSF (USA).

107 References

- 108 [1] **D0** Collaboration, B. Abbott et al. *Phys. Rev. Lett.* **82** (1999) 2457.
- 109 [2] E. Eichten, K. D. Lane, and M. E. Peskin *Phys. Rev. Lett.* **50** (1983) 811.
- 110 [3] U. Baur, I. Hinchliffe, and D. Zeppenfeld *Int. J. Mod. Phys.* **A2** (1987) 1285.
- 111 [4] **CMS** Collaboration, R. Adolphi et al. *JINST* **0803** (2008) S08004.
- 112 [5] **CMS** Collaboration, G. L. Bayatian et al. CERN-LHCC-2006-001.
- 113 [6] G. P. Salam and G. Soyez *JHEP* **05** (2007) 086.
- 114 [7] **GEANT4** Collaboration, S. Agostinelli et al. *Nucl. Instrum. Meth.* **A506** (2003) 250.
- 115 [8] **CMS** Collaboration *CMS Physics Analysis Summary* **JME-07-002** (2008).
- 116 [9] **CMS** Collaboration *CMS Physics Analysis Summary* **JME-07-003** (2008).
- 117 [10] R. D. Cousins, K. E. Hymes, and J. Tucker [arXiv:0905.3831](https://arxiv.org/abs/0905.3831).
- 118 [11] C. J. Clopper and E. S. Pearson *Biometrika* **26** (1934), no. 4, 404.
- 119 [12] **CMS** Collaboration *CMS Physics Analysis Summary* **JME-08-003** (2009).
- 120 [13] T. Sjostrand, L. Lonnblad, and S. Mrenna [arXiv:hep-ph/0108264](https://arxiv.org/abs/hep-ph/0108264).
- 121 [14] Z. Nagy *Phys. Rev.* **D68** (2003) 094002.
- 122 [15] J. Pumplin et al. *JHEP* **07** (2002) 012.
- 123 [16] **CDF** Collaboration, T. Aaltonen et al. *Phys. Rev.* **D79** (2009) 112002.

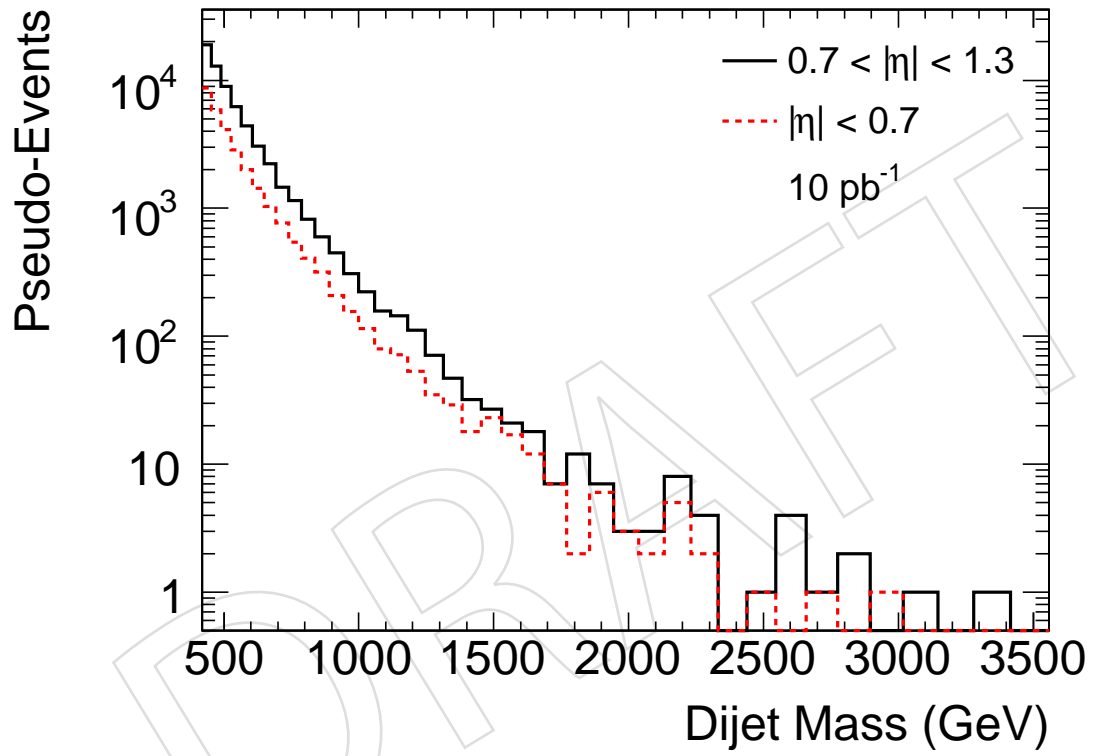


Figure 1: The number of observed events as a function of dijet mass for $|\eta| < 0.7$ (dashed) and for $0.7 < |\eta| < 1.3$ (solid). WARNING: CMS DATA IN THIS FIGURE IS FAKE

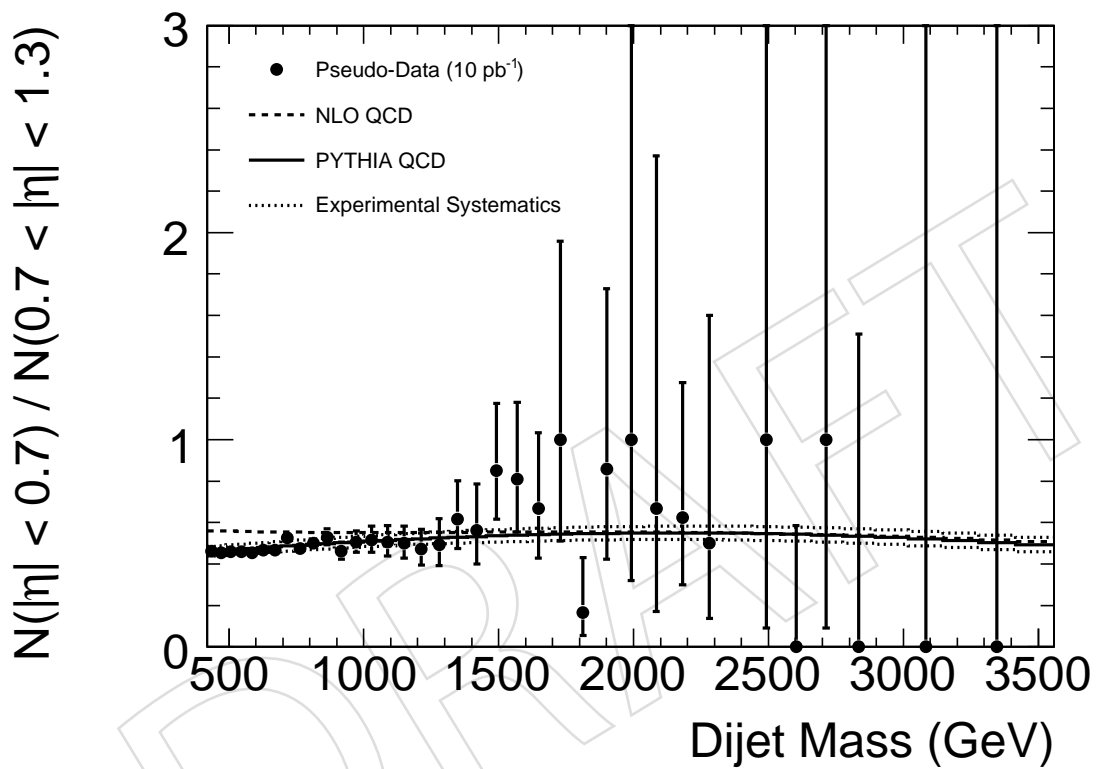


Figure 2: The dijet ratio as a function of dijet mass (points) is compared to a simulation of QCD and the CMS detector (solid curve) and a next-to-leading order QCD calculation (dashed curve). The error bars show the statistical uncertainty on the data and the dotted curves show the experimental systematic uncertainty centered on a smooth fit to the data. WARNING: CMS DATA IN THIS FIGURE IS FAKE

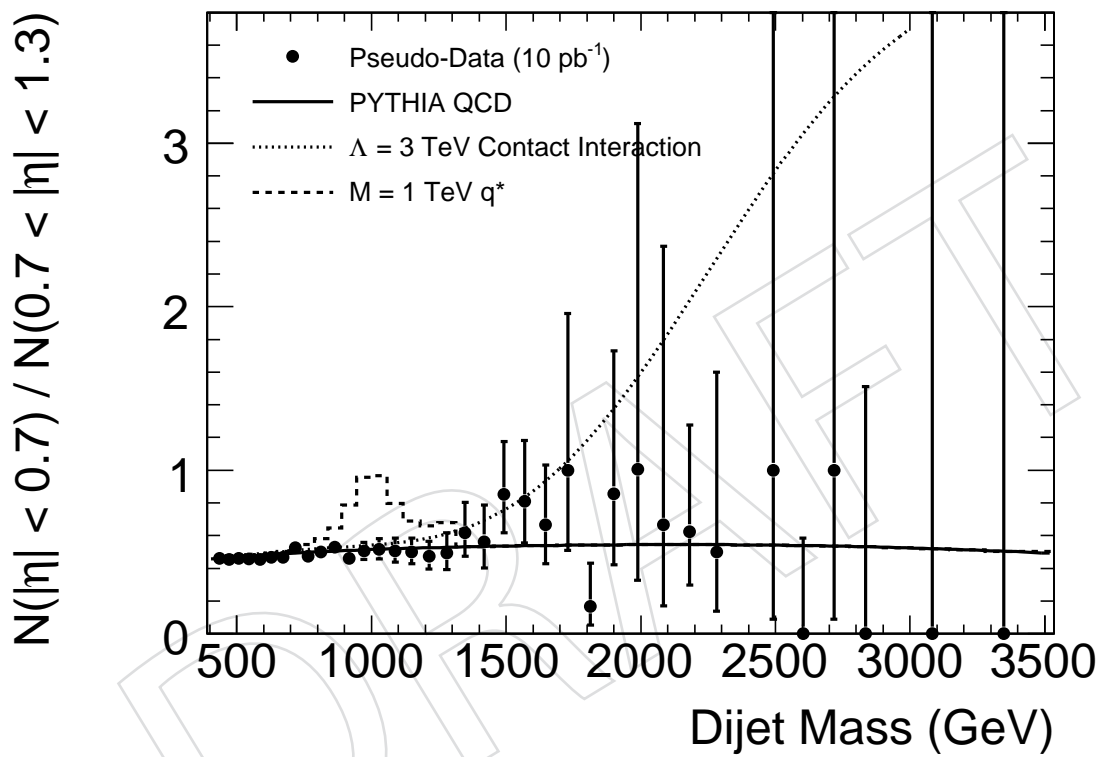


Figure 3: The dijet ratio as a function of dijet mass (points) is compared to QCD (solid curve) and a contact interaction with scale $\Lambda = 3$ TeV (dotted curve) and an excited quark with mass 1 TeV (dashed histogram). WARNING: CMS DATA IN THIS FIGURE IS FAKE

Table 1: For each bin of dijet mass we list the numerator and denominator of the dijet ratio, followed by the measured ratio and its upper and lower statistical uncertainty. WARNING: CMS DATA IN THIS TABLE IS FAKE

mass range (GeV)	ratio	+ error	- error
419 - 453	8713 / 18918 = 0.461	0.00604	0.00596
453 - 489	5876 / 12923 = 0.455	0.00727	0.00715
489 - 526	4126 / 8967 = 0.460	0.00882	0.00866
526 - 565	2863 / 6238 = 0.459	0.0106	0.0104
565 - 606	2003 / 4422 = 0.453	0.0125	0.0122
606 - 649	1429 / 3061 = 0.467	0.0154	0.0150
649 - 693	1039 / 2220 = 0.468	0.0183	0.0176
693 - 740	767 / 1459 = 0.526	0.0245	0.0234
740 - 788	546 / 1152 = 0.474	0.0259	0.0246
788 - 838	409 / 818 = 0.500	0.0322	0.0302
838 - 890	316 / 597 = 0.529	0.0395	0.0368
890 - 944	208 / 450 = 0.462	0.0422	0.0388
944 - 1000	156 / 309 = 0.505	0.0547	0.0494
1000 - 1058	115 / 223 = 0.516	0.0664	0.0590
1058 - 1118	80 / 158 = 0.506	0.0798	0.0691
1118 - 1181	72 / 144 = 0.500	0.0835	0.0717
1181 - 1246	53 / 112 = 0.473	0.0933	0.0783
1246 - 1313	35 / 71 = 0.493	0.125	0.101
1313 - 1383	29 / 47 = 0.617	0.185	0.143
1383 - 1455	18 / 32 = 0.563	0.224	0.162
1455 - 1530	23 / 27 = 0.852	0.324	0.235
1530 - 1607	17 / 21 = 0.810	0.371	0.255
1607 - 1687	12 / 18 = 0.667	0.366	0.239
1687 - 1770	7 / 7 = 1.00	0.958	0.489
1770 - 1856	2 / 12 = 0.167	0.264	0.113
1856 - 1945	6 / 7 = 0.857	0.872	0.435
1945 - 2037	3 / 3 = 1.00	2.11	0.679
2037 - 2132	2 / 3 = 0.667	1.704	0.494
2132 - 2231	5 / 8 = 0.625	0.652	0.326
2231 - 2332	2 / 4 = 0.500	1.10	0.362
2332 - 2438	0 / 0 = —	0.00	0.00
2438 - 2546	1 / 1 = 1.00	10.1	0.910
2546 - 2659	0 / 4 = 0.00	0.584	0.00
2659 - 2775	1 / 1 = 1.00	10.1	0.910
2775 - 2895	0 / 2 = 0.00	1.51	0.00
2895 - 3019	1 / 0 = —	0.00	0.00
3019 - 3147	0 / 1 = 0.00	5.30	0.00
3147 - 3279	0 / 0 = —	0.00	0.00
3279 - 3416	0 / 1 = 0.00	5.30	0.00